Granulocyte Colony-Stimulating Factor-Induced TAF9 Modulates P53-TRIAP1-CASP3 Axis to Prevent Retinal Ganglion Cell Death after Optic Nerve Ischemia

Yao-Tseng Wen
Buddhist Tzu Chi General Hospital Hualien: Hualien Tzu Chi Hospital
Keh-Liang Lin
Chung Shan Medical University Hospital
Chin-Te Huang
Tzu Chi University
Rong Kung Tsai (rktsai@tzuchi.com.tw)
Hualien Tzu Chi Hospital https://orcid.org/0000-0001-8760-5739

Research article

Keywords: Granulocyte colony-stimulating factor, Rat anterior ischemic optic neuropathy model, Retinal ganglion cell, TBP associated factor 9, TP53, TRIAP1

Posted Date: January 6th, 2021

DOI: https://doi.org/10.21203/rs.3.rs-138908/v1

Abstract

Background

Optic nerve head (ONH) infarct can result in progressive retinal ganglion cell (RGC) death. Some evidences indicated that the granulocyte colony-stimulating factor (GCSF) provides positive effects against ischemic damage on RGCs. However, protective mechanisms of the GCSF after ONH infarct are complex and remain unclear.

Methods

To investigate the complex mechanisms, the transcriptome profiles of the GCSF-treated retinas were examined using microarray technology. The retinal mRNA samples on days 3 and 7 post rat anterior ischemic optic neuropathy model (rAION) were analyzed by microarray and bioinformatics analyses. To evaluate the TAF9 function in RGC apoptosis, GCSF plus TAF9 siRNA-treated rats were evaluated using retrograde labeling with FluoroGold assay, TUNEL assay, and Western blotting in a rAION.

Results

GCSF treatment influenced 3101 genes and 3332 genes on days 3 and 7 post rAION, respectively. ONH infarct led to changes in 702 and 179 genes on days 3 and 7 post rAION, respectively. After cluster analysis, the TATA box-binding protein (TBP)-associated factor levels were significantly reduced after ONH infarct but significantly increased after GCSF treatment. The network analysis revealed that TBP associated factor 9 (TAF9) can bind to TP53 to induce TP53 regulated inhibitor of apoptosis 1 (TRIAP1) expression. The RGC density in the GCSF plus TAF9 siRNA-treated group was 1.95-fold (central retina) and 1.75-fold (midperipheral retina) lower than that in the GCSF-treated group ($p < 0.05$). The number of apoptotic RGC in the GCSF plus TAF9 siRNA-treated group is threefold higher than that in the GCSF-treated group ($p < 0.05$). Treatment with TAF9 siRNA significantly reduced GCSF-induced TP53 and TRIAP1 expression by 2.4-fold and 4.7-fold, respectively, in the rAION model. Overexpression of TAF9 significantly reduced apoptotic RGC and CASP3 levels and induced TP53 and TRIAP1 expression in the rAION model.

Conclusion

Our in vivo study is the first to report that GCSF is able to induce TAF9 expression to control RGC death and survival after ON infarct. Besides, the binding of TAF9 and TP53 is crucial to inhibit TP53 degradation and to modulate TRIAP1-CASP3 axis. Thus, we considered that TAF9 is a potential drug for patient with NAION.

Background

In elderly individuals, the most common type of acute optic neuropathy is non-arteritic anterior ischemic optic neuropathy (NAION), with an estimated annual incidence of 3.72 per 100,000 individuals in Taiwan

[1]. NAION is defined clinically as painless visual loss with swelling of the optic disc leading to optic disc atrophy [2]. Currently, there is no effective treatment for NAION. Optic nerve (ON) ischemia induces a series of detrimental events, eventually resulting in retinal ganglion cell (RGC) loss [2]. RGC death and axon degeneration are major complications of ischemic damage and mainly caused by oxidative stress [3-6], pro-inflammatory factors [6, 7], aberrant calcium ion homeostasis [8], and macrophage polarization [7, 9]. Therefore, a comprehensive investigation on the complex molecular mechanisms of axonal degeneration and RGC death in ON ischemia may bring new horizon for treatment.

Several efforts in preventing ON injuries and RGC death have been made using different approaches, such as anti-inflammatory compounds [10, 11], neurotropic factors [12, 13], oxidative stress regulators [5], calcium channel blockers [14], microglial activation inhibitors [7, 15], and blood-borne macrophage infiltration blockers [7, 12, 16]. These potential treatments provide some possible directions to elucidate how to control the fate of RGCs. In context with our previous study on neuroprotective effects of granulocyte-colony stimulating factor (GCSF), we found that GCSF exhibited the ability to rescue RGC from apoptosis, which may be involved in modulations of blood-ON barrier, macrophage infiltration, and inflammatory reaction [7]. Moreover, our previous findings demonstrated that treatment with GCSF can activate PI3K/AKT pathway to protect RGC from apoptosis [17].

GCSF belongs to a member of the hematopoietic growth factor family. It is widely used in clinical practice for the treatment of neutropenia [18]. Recent findings have suggested that GCSF also has a nonhematopoietic role in memory improvement in Alzheimer's disease and neuroprotective role in Parkinson's disease [19, 20]. It also promotes angiogenesis and inhibits apoptosis and inflammation in rats with ischemic stroke [21-23]. Furthermore, the GCSF receptor (GCSFR) is expressed in various neural and glial cells, such as RGCs, microglia, astrocyte, and oligodendrocyte, which results in direct activation of GCSFR signaling pathways, including JAK/STAT, PI3K/AKT, and MAPK/ERK pathways [24]. These signaling pathways are involved in cell growth and differentiation. Thus, the mechanisms by which GCSF promotes RGC survival are likely complex.

To reveal these complex mechanisms, transcriptome analysis of the rat retina is a possible approach that can be used to investigate the transcriptome changes after ON infarct with or without GCSF treatment. The microarray technique is a high throughput analysis to determine the expression level of large numbers of genes simultaneously. This technique has also been used to evaluate changes after axonal injury in both the retina and isolated RGCs [25, 26]. Therefore, we considered that microarray analysis is an adequate tool to explore any possible mechanism involved in RGC apoptosis and survival.

Different animal models have been used to investigate RGC pathology. Herein, we used rat anterior ischemic optic neuropathy (rAION) model as it represents similar features and pathology with human and primate AION [27]. The rAION model is achieved by photodynamic therapy, which generates superoxide radicals in the ON capillaries, causing capillary thrombosis, inflammation, and oxidative stress [27]. These pathological changes are important events to induce RGC apoptosis. Thus, it is an appropriate model to use in investigating the mechanisms of RGC apoptosis.

In present study, a comparative microarray analysis was adopted to explore the dynamic transcriptome changes in the rat retina under ON infarct and GCSF treatment. We identified that the mRNA levels of several TATA-box binding protein (TBP)-associated factors (TAFs) were significantly reduced after ONH infarct but significantly increased after GCSF treatment. Among these genes, we targeted one gene, transcription initiation factor TFIID subunit 9 (*taf9*), which encodes for one of the smaller subunits of transcription factor IID (TFIID) that binds to the general transcription factor transcription initiation factor IIB (Gtf2b) and several transcriptional activators, such as p53 and Vp16 [28, 29]. Taf9 physically interacts with p53 at its N-terminus, where p53 also interacts with its negative regulator, Mdm2, thereby inhibiting Mdm2 degradation of p53 [30]. Functionally, this interaction translates to an increase in p53-induced angiogenesis, DNA repair, cell arrest, cell survival, or apoptosis [30]. However, it is questionable whether TAF9 drives P53 toward cell survival or apoptosis. Thus, this study aimed to reveal the underlying mechanisms of TAF9 in RGC apoptosis and cell survival.

Materials And Methods

Study design

In examining the transcriptome profiles in the retina, the rAION-inducted rats were treated by PBS or GCSF. At day 3 post rAION, the retina samples were collected in the PBS-treated group (n = 3) and GCSF-treated group (n = 3). At day 7 post rAION, the retina samples were again collected in the PBS-treated group (n = 3) and GCSF-treated group (n = 3). The retina samples in the sham-operated group (n = 3) were also collected. All retina samples were used to extract the mRNA. The mRNA samples were analyzed by RNA microarray to profile the transcriptome in each group. The differentially expressed genes were classified by GO analysis. Among the differentially expressed genes, the TBP-associated proteins were classified into the function of cell growth. Therefore, the TBP-associated proteins were selected to predict the protein-to-protein interaction by network analysis (STRING 9.0). The TP53 was predicted to interact with many TBP-associated proteins in the network analysis. One of the TBP-associated proteins, TAF9, was selected to be the target protein to verify the function in the regulation of cell death and survival. TAF9 knockdown and overexpression experiments were performed in the rAION model. The rAION-inducted rats were treated with scramble siRNA, GCSF plus scramble siRNA, and GCSF plus TAF9 siRNA to evaluate the visual function (n = 12 in each group), RGC density (n = 12 in each group), and apoptotic RGCs (n = 6 in each group). The TAF9, TP53, and TRIAP1 levels were evaluated in each group (n = 6) using Western blot analysis. Moreover, the AAV2-mediated overexpression of TAF9 was intravitreally administered before rAION induction to examine the anti-apoptotic ability of TAF9 in the rAION model. The number of apoptotic RGCs was evaluated in the AAV2-r-TAF9-treated group (n = 6) and PBS-treated group (n = 6). The TP53, TRIAP1, and cleaved-CASP3 levels were determined in the AAV2-r-TAF9-treated group (n = 3) and PBS-treated group (n = 3).

Animals

Male Wistar rats were used in the study. The rats were aged 6-8 weeks with body weight of 150–180 g. Animal care and experimental procedures were performed in accordance with the Association for Research in Vision and Ophthalmology Statement for the Use of Animals in Ophthalmic and Vision Research, and the Institutional Animal Care and Use Committee (IACUC) at the Tzu Chi Medical Center approved all animal experiments.

rAION induction

The procedure of rAION induction was described in our previous study [31]. Before general anesthesia, all rats were administered Mydrin-P (Santan, Shiga, Japan) and Alcaine (Alcon, Texas, USA) eye drops for pupil dilation and topical anesthesia, respectively. Subsequently, the rats were injected intramuscularly by a mixture of ketamine (40 mg/kg body weight, Pfizer, UK) and xylazine (4 mg/kg body weight; Sigma, St. Louis, MO, USA) for general anesthesia. For photosensitization, 2.5 mM Rose Bengal diluted in PBS (1 ml/kg of body weight) was administered intravenously before laser application. After rose bengal injection, the optic disc was immediately exposed to an argon green laser system (MC-500 Multi-color laser, Nidek Co., Ltd, Tokyo, Japan, setting: 532 nm wavelength, 500 μm size and 80 mW power) for 12 1-s pulses. A laser fundus lens (Ocular Instruments, Inc.) was used to target the optic disc. At the end of experiment, TobraDex eye ointment (Alcon-Couvreur, Puurs-Sint-Amands, Belgium) was applied to the eyes of all experimented rats.

RNA microarray analysis (quality check, annotation, and ontology)

The retina samples were collected at days 3 and 7 post rAION. Total RNA was isolated from retina homogenate using TRIzol reagent (Invitrogen) according to the manufacturer's instructions. Complementary DNAs were synthesized using reverse transcriptase kit. RNA microarray analysis was performed using Rat OneArray kit according to the manufacturer's protocol. Clustering and principal component analysis were performed to determine the differences among biological sample replicates and their treatment conditions. Raw intensities were normalized with median scaling normalizing method, and covariance was determined by error model of Rosetta Resolver system. Normalized intensity was transformed to the $\log_2$ ratio (fold change). Gene annotation was performed with reference to NCBI RefSeq Release 57. EnsEMBL released 70 cDNA sequences and rattus_norvegicus_core_70_5b annotations. Differentially expressed genes that showed both a log2 ratio (fold change) >1 and $p < 0.05$ were considered candidate genes.

FVEP recordings

FVEP measurements were performed as described in our previous study [31]. After general anesthesia, the sagittal region of the skull was opened in the rats. The 4-mm screw implants were passed through the

skull approximately 1.5 mm and placed at the frontal cortex and primary visual cortex region of both hemispheres using stereotaxic coordinates. A visual electrodiagnostic system (Diagnosys LLC, Lowell, MA, USA) was used to measure the FVEP. The number of sweeps per average was 64 for each rat. A comparison of the average amplitude of the P1-N2 wave in each group was made to evaluate visual function.

Retrograde labeling of RGCs and measurement of RGC density

RGCs were labeled as described in our previous study [31]. Briefly, retrograde tracer dye fluorogold was injected into the superior colliculus one week before the rats were euthanized. One week after labeling, the rats were euthanized, and retinas were carefully flat mounted. The central and midperipheral regions in the retina were examined under a fluorescence microscope with a built-in filter set (excitation filter, 350–400 nm; barrier filter, 515 nm) and connected digital imaging system. RGC density was calculated using ImageMaster 2D Platinum Software V 7.0 (GE Healthcare, Illinois, USA).

Retinal and ON sample preparation

After euthanized, there rat eyeballs were fixed in 4% paraformaldehyde overnight. The eyecups and ONs were separated and transferred to 30% sucrose solution; the samples were incubated at 4°C until they settled at the bottom of the tubes. The retina cross-section and ON longitudinal sections of 15 μm were obtained using a cryostat.

TUNEL assay

To ensure the use of equivalent fields for comparison, all frozen retinal sections were prepared with a 1–2 mm distance from the ON head. We counted apoptotic cells using the TUNEL assay kit (Click-iT™ Plus TUNEL Assay, Invitrogen, Waltham, USA). Nuclei were stained with 4t,6-diamidino-2-phenylindole (DAPI). The TUNEL-positive cells in the RGC layer of each sample were counted in 10 high power field (HPF) (400×), and an average of three sections per retina was used for further analysis (n = 6 rats per group).

Western blotting

After euthanized, and the rats' eyes were enucleated. The retinas were homogenized in lysis buffer. The protein sample was separated on 10% bis-acrylamide gel. The proteins were transferred to polyvinylidene difluoride (PVDF) membranes. The membranes were blocked with 5% non-fat dry milk for 1 h. The membranes were incubated with Taf9, TP53, TRIAP1, CASP3, ACTIN antibody at 4°C for 12–16 h, followed by incubation with a secondary antibody conjugated to HRP against the appropriate host

species for 1 h at room temperature. Then, the membranes were developed using enhanced chemiluminescent (ECL) substrate. Membranes were exposed to a Western blot analyzer, and the relative density was calculated using image master platinum software V 7.0 (GE Healthcare, Illinois, USA).

Statistical analysis

All statistical analyses were performed using IBM SPSS software. The data are presented as mean ± standard deviation. A Mann–Whitney U test was used for comparisons between groups. P-values < 0.05 were considered statistically significant, with * representing $p \leq 0.05$.

Results

Identification of differentially expressed genes by microarray

To investigate RGC death and survival in the transcriptional level, the rAION-inducted rats were treated with phosphate buffered saline (PBS) or GCSF. The transcriptome profiles were analyzed using oligonucleotide microarrays. Microarray data were analyzed using the Gene Expression Pattern Analysis Suite to identify the differentially expressed genes. In a total of 24,358 analyzed genes, 3101 and 3332 transcripts were regulated by GCSF treatment on days 3 and 7 post rAION, respectively. In addition, 702 and 179 transcripts were regulated by PBS treatment on days 3 and 7 post rAION, respectively (Figure 1A–D). Unsupervised hierarchical clustering analysis of differentially expressed genes from all groups was conducted to investigate the similarity of the whole gene expression between the experimental samples. The result indicated that the profile of gene expression in the GCSF-treated group was similar (Figure 1E). Additionally, the PBS-treated rats on days 3 and 7 post rAION also exhibited similar gene expression. As stated above, the trend of gene expression is consistent between the PBS- and GCSF-treated groups.

TAFs involved in regulation of cell death and proliferation

To classify the biological function of differentially expressed genes, we employed a gene ontology (GO) analysis. After GO analysis, there were many TBP-associated proteins that are classified into the category of regulation of cell death and proliferation. We found that 18 TAFs, including TAF1, TAF1a, TAF1b, TAF1c, TAF1d, TAF2, TAF5, TAF6l, TAF7, TAF7l, TAF8, TAF9, TAF9b, TAF10, TAF11, TAF12, TAF13, and TAF15, were upregulated by GCSF treatment. Additionally, 17 TAFs, including TAF1, TAF1a, TAF1b, TAF1c, TAF1d, TAF3, TAF5, TAF6, TAF6l, TAF7, TAF7l, TAF8, TAF9, TAF10, TAF11, TAF12, and TAF13, were downregulated by PBS treatment (Figure 2). It indicated that the expression level of many TAFs was suppressed by ON ischemic injury and induced by GCSF treatment.

Network analysis revealed that TAFs directly interact with TP53 and TBP

STRING network analysis exhibited that many TAFs interact directly with TP53, including TAF1, TAF1L, TAF2, TAF3, TAF4, TAF5, TAF6, TAF7, TAF7L, TAF9, TAF9b, TAF10, TAF11, TAF12, and TAF13 (Figure 3). Additionally, TAFs have direct interaction with TBP, including TAF1, TAF1a, TAF1b, TAF1c, TAF1d, TAF1L, TAF2, TAF3, TAF4, TAF5, TAF6, TAF7, TAF7L, TAF9, TAF9b, TAF10, TAF11, TAF12, and TAF13. Among these TAFs, TAF9 was predicted to bind with TP53, and the expression level of TAF9 was dramatically elevated by GCSF treatment and suppressed by PBS treatment. The biological function of TAF9 is involved in gene regulation associated with apoptosis [32]. Thus, we selected TAF9 as a candidate gene to evaluate its function in RGC apoptosis and survival after ON ischemia.

Taf9 knockdown impaired the protective effect of GCSF on the visual function

To evaluate the role of TAF9 in the protection of visual function in rAION, flash visually evoked potentials (FVEPs) were measured at day 28 post infarct (Figure 4A). On TAF9 knockdown, we found no improvement in visual function despite GCSF treatment. The P1-N2 amplitudes in the sham-operated, scramble siRNA-treated, GCSF plus scramble siRNA-treated, and GCSF plus TAF9 siRNA-treated groups were 65.8 ± 12.7 μV, 23.4 μV ± 4.2 μV, 49.5 ± 6.6 μV, and 28.9 ± 8.4 μV, respectively (Figure 4B). Treatment with GCSF plus TAF9 siRNA reduced the P1-N2 amplitude by 1.71-fold compared to treatment with GCSF plus scramble siRNA (Figure 4B, $p < 0.05$).

Taf9 knockdown impaired the protective effect of GCSF on RGC density

In the central retina, the RGC density in the sham-operated, scramble siRNA-treated, GCSF plus scramble siRNA-treated, and GCSF plus TAF9 siRNA-treated groups were 1402.5 ± 99.1, 655.2 ± 199.6, 1265.1 ± 352.5, and 649.7 ± 227.6 cells/mm^2, respectively (Figure 5A). In the midperipheral retina, the RGC densities in the sham-operated, scramble siRNA-treated, GCSF plus scramble siRNA-treated, and GCSF plus TAF9 siRNA-treated groups were 1219.4 ± 201.3, 319.2 ± 195.8, 863.3 ± 161.3, and 492.9 ± 250.1 cells/mm^2, respectively (Figure 5A). The RGC density in the GCSF plus TAF9 siRNA-treated group was significantly reduced by 1.94- and 1.75-fold in the central and midperipheral retinas, respectively, compared with that in the GCSF plus scramble siRNA-treated group (Figure 5B, $p < 0.05$).

TAF9 knockdown impaired the anti-apoptotic ability of GCSF

The numbers of $TUNEL^+$ cells in the sham-operated, scramble siRNA-treated, GCSF plus scramble siRNA-treated, and GCSF plus TAF9 siRNA-treated groups were 0.2 ± 0.4/HPF, 7.4 ± 2.7/HPF, 2.1 ± 1.3/HPF, and 6.3 ± 2.2/HPF, respectively. The number of $TUNEL^+$ cell in the GCSF plus TAF9 siRNA-treated group

significantly increased by threefold compared to that in the GCSF plus scramble siRNA-treated group ($p < 0.05$), but there was no significant difference between the scramble siRNA-treated and GCSF plus TAF9 siRNA-treated groups (Figure 6), further suggesting a survival pathway dependent on TAF9.

TAF9 knockdown suppressed GCSF-induced TP53 and TRIAP1 expression

Western blotting confirmed that the GCSF plus scramble siRNA-treated group exhibited the highest protein level of TAF9 compared with other groups (Figure 7, $p < 0.05$). GCSF plus TAF9 siRNA treatment significantly repressed TAF9 protein expression by 6.9-fold compared to GCSF plus scramble siRNA treatment ($p < 0.05$). In the GCSF plus TAF9 siRNA-treated group, the TP53 level was reduced by 2.4-fold compared to that in the GCSF plus scramble siRNA-treated group ($p < 0.05$). One of TP53 regulated genes, TP53-regulated inhibitor of apoptosis gene 1 (TRIAP1), can inhibit apoptosis through interaction with APAF1 and heat shock protein 70 (HSP70) complex [33]. Our Western blotting data demonstrated that the TRIAP1 level was reduced by 4.7-fold in the GCSF plus TAF9 siRNA-treated group compared with that in the GCSF plus scramble siRNA-treated group ($p < 0.05$).

Overexpression of TAF9 inhibited RGC death by modulating TP53-TRIAP1-CASP3 axis

To explore the role of TAF9 in the regulation of RGC death and survival, the AAV2-rTAF9 was used to overexpress the TAF9 level in the rAION model. Four weeks after rAION, the numbers of TUNEL positive cells in the PBS-treated and AAV2-r-TAF9-treated groups were 7.4 ± 2.7/HPF and 2.4 ± 1.7/HPF, respectively (Figure 8A). The number of TUNEL positive cell was 3.1-fold lower in the AAV2-r-TAF9-treated group than that in the PBS-treated group ($p < 0.05$). Western blotting confirmed that the TP53 and TRIAP1 levels in the AAV2-r-TAF9-treated group were significantly increased by 2.04- and 2.71-fold, respectively, compared to those in the PBS-treated group (Figure 8B, $p < 0.05$). Moreover, the cleaved-caspase 3 (Cl-casp3) level was reduced by 2.33-fold in the AAV2-rTAF9-treated group compared to that in the PBS-treated group (Figure 8B, $p < 0.05$).

Discussion

In this study, we conducted a microarray analysis of rat retinas to compare the differences between PBS and GCSF treatments after rAION induction to profile the retinal transcriptomes in response to ON ischemic injury or RGC protective environment. Dynamic transcriptome profiling revealed many novel differentially expressed genes involved in the regulation of cell death and proliferation. Among these transcripts, some genes involved in the regulation of cell death and proliferation are the TAFs. Besides, a subsequent in silico pathway analysis revealed significant interactions between TAFs and TP53. One TP53 coactivator, TAF9, was selected to prove its role in the regulation of RGC death and survival because TAF9 is an apoptosis regulator [34]. TAF9 knockdown not only effectively reduced the neuroprotective effects of GCSF but also inhibited G-CSF-induced TP53 and TRIAP1 expressions in the

rAION model. In corresponding to the findings of TAF9 knockdown, overexpression of TAF9 in the rAION model induced the levels of TP53 and TRIAP1 and suppressed the level of cleaved-CASP3, which provided an anti-apoptotic effects on RGCs. Thus, we suggested that TAF9 is a key element in modulating the TP53-TRIAP1-CASP3 pathway to control RGC death and survival. This transcriptomic analysis discovered a novel GCSF-regulated pathway, which is involved in RGC death and survival.

The differentially expressed genes found in the study are involved in the regulation of RGC death. Notably, ON ischemia influenced 702 and 179 transcripts on days 3 and 7 post rAION, respectively. We found that the numbers of ON ischemia-influenced genes are gradually reduced from days 3 to 7 post rAION. These data indicated that a dramatic change in transcription occurs in the acute stage, but this transcriptional change returns to normal in the subacute stage. A similar observation was found in our previous study that vascular permeability was highly increased in the acute stage and reduced in the subacute stage after ON infarct [7]. Taken together, we considered that ON ischemia may cause severe pathological changes in the acute stage and the natural course of recovery may be started in the subacute stage. Therefore, the therapeutic window should be focused on the acute stage in ON ischemia. As expected, our previous findings also demonstrated that early treatment with GCSF or methylprednisolone provided good neuroprotective effects in the rAION model [7, 35].

Comparing the GCSF-treated groups with the PBS-treated groups, GCSF treatment constantly influenced > 3000 transcripts for 7 days, but the PBS-treated rats gradually reduced the transcriptional changes from the acute to subacute stage. It indicated that immediate treatment with GCSF can influence several genes to trigger the rescue actions after ON ischemia. This remarkable transcriptional changes provided informative messages in discovering the key pathways involved in RGC survival. In this transcriptomic analysis, we found that many TBP-associated proteins were suppressed by ischemic insult but induced by GCSF treatment. These TAFs were involved in the regulation of RGC death and survival. At the molecular level, gene expression is regulated by many core transcriptional complexes, such as TFIID, along with different cofactors [36]. Previous studies revealed TFIID as an integral component of the core transcriptional machinery for RNA polymerase II at mRNA encoding genes [36, 37] and demonstrated that it is assembled with TBP and multiple TAFs [38]. To date, many TAFs and several tissue-specific variants are characterized [39]. Some genetic studies revealed the complex role of TFIID in controlling tissue-specific and context-dependent transcriptional processes, proving the existence of different TFIID complexes and tissue-specific TAFs [40-44]. TFIID subunits regulate many cellular processes in tissue-specific manners, which facilitated research into TAF involvement in moderating biological functions, including proliferation, differentiation, apoptosis, metastasis, and hormone response [45].

After network analysis, we found that TAF9 was predicted to interact with TBP and TP53. In addition, TAF9 was highly upregulated by GCSF treatment at days 3 and 7 post rAION. It implied that TAF9 plays an important role in modulating RGC death and survival via P53 signaling pathway. TAF9 was reported to be a crucial P53 coactivator for stabilization and activation of P53 [28, 30]. TAF9 inhibits MDM2-mediated degradation of p53 by reducing MDM2 binding to p53 [30]. A previous study also demonstrated that one TFIID complex lacking TAF9 in Hela cells causes apoptosis [46]. Interruption of interactions

between Hedgehog transcription factors (Gli proteins) and TAF9 reduces Gli/TAF9-dependent transcription, suppresses cancer cell proliferation, and reduces xenograft growth [34]. As mentioned above, we hypothesize that the high TAF9 level activates P53 pathway to inhibit RGC apoptosis after ON infarct. To verify our hypothesis, the TAF9-knockdown experiment was performed to discover the role of TAF9 in the regulation of RGC death and survival. As expected, TAF9 knockdown effectively reduced the protective effects of GCSF in the rAION model. Therefore, we demonstrated that TAF9 plays a key role in RGC protection after ON ischemia.

Cell apoptosis is manipulated on multiple levels by the sequence-specific transcription factor TP53, with > 100 genes existing TP53 binding sites [47]. Moreover, the function of these genes remains unclear. One of these genes is TP53-regulated inhibitor of apoptosis gene 1 (TRIAP1), which has a p53 binding site within its coding sequence and is upregulated in many cancer cells [48]. TRIAP1 was reported to protect cancer cells from apoptosis through interaction with HSP70 or repression of cyclin-dependent kinase inhibitor 1 (p21) [49, 50]. Recent findings demonstrated that TRIAP1 contributes to the resistance of apoptosis in a mitochondria-dependent manner [51, 52]. Based on these evidences, we further evaluated the relationship among TAF9, P53, TRIAP1, and CASP3 in the rAION model. Remarkably, immunoblotting data demonstrated that TAF9 overexpression prevented TP53 degradation and increased TRIAP1 expression in the rAION model. Additionally, we found that TAF9 overexpression reduced apoptotic RGCs and caspase 3 level after ON infarct. Taken together, we suggested that TAF9 plays a key role in the protection of ischemia-induced RGC apoptosis by modulation of TP53-TRIAP1-CASP3 axis.

Conclusion

Therefore, our transcriptomic analysis found a novel signaling pathway to elucidate the anti-apoptotic effects of GCSF on RGCs. In this novel signaling pathway, TAF9 is a key element in the modulation of TP53-TRIAP1-CASP3 axis for preventing RGC death. All the evidences suggest that TAF9 is a potential target in developing a new drug for NAION treatment.

Abbreviations

GCSF: granulocyte colony-stimulating factor; Gli: hedgehog transcription factors Gtf2b; general transcription factor transcription initiation factor IIB; IACUC: Institutional Animal Care and Use Committee; NAION: non-arteritic anterior ischemic optic neuropathy; ONH: Optic nerve head; rAION: rat anterior ischemic optic neuropathy model; RGC: retinal ganglion cell; TBP: TATA box-binding protein; TAF9: TBP associated factor 9; TRIAP1: TP53 regulated inhibitor of apoptosis 1; TF IID: transcription factor IID

Declarations

Ethical Approval and Consent to participate

Animal care and experimental procedures were performed in accordance with the Association for Research in Vision and Ophthalmology Statement for the Use of Animals in Ophthalmic and Vision Research, and the Institutional Animal Care and Use Committee (IACUC) at the Tzu Chi Medical Center approved all animal experiments.

Consent for publication

Not applicable.

Availability of supporting data

Raw data can be obtained from corresponding authors.

Competing interests

The authors declare no competing interests

Funding

This study was supported by a Ministry of Science and Technology Grant from the Taiwanese Government (MOST 103-2314-B-303-007-MY3).

Author contributions

Y-T W and R-K T designed the experiments. Y-T W performed the experiment. C-T H, K-L L, and Y-T W analyzed the data. R-K T contributed the reagents/materials/ analysis tools. C-T H, Y-T W and R-K Tsai wrote the manuscript. All contributing authors have read and approved the final version of the manuscript.

Acknowledgments

The authors sincerely thank Mr. Yu-Chieh Ho, Mr. Kishan Kapupara, and Mrs. Su-Chen Chen for the technical assistance with experiments and data collection. This study was supported by a grant from the Ministry of Science and Technology, Taiwan (MOST 103-2314-B-303-007-MY3).

Author information

Affiliations:

Institute of Eye Research, Hualien Tzu Chi Hospital, Buddhist Tzu Chi Medical Foundation, Hualien, Taiwan.

Yao-Tseng Wen, Chin-Te Huang, and Rong-Kung Tsai

Department of Medical laboratory and Biotechnology, Chung Shan Medical University, Taichung, Taiwan.

Keh-Liang Lin

Department of Ophthalmology, Chung Shan Medical University Hospital, College of Medicine, Chung Shan Medical University, Taichung, Taiwan.

Chin-Te Huang

Institute of Medical Sciences, Tzu Chi University, Hualien, Taiwan.

Chin-Te Huang and Rong-Kung Tsai

Corresponding author:

Correspondence to Rong-Kung Tsai

References

1. Lee YC, Wang JH, Huang TL, Tsai RK: Increased Risk of Stroke in Patients With Nonarteritic Anterior Ischemic Optic Neuropathy: A Nationwide Retrospective Cohort Study.*Am J Ophthalmol* 2016, 170:183-189.
2. Bernstein SL, Johnson MA, Miller NR: Nonarteritic anterior ischemic optic neuropathy (NAION) and its experimental models.*Prog Retin Eye Res* 2011, 30:167-187.
3. Yang Y, Xu C, Chen Y, Liang JJ, Xu Y, Chen SL, Huang S, Yang Q, Cen LP, Pang CP, et al: Green Tea Extract Ameliorates Ischemia-Induced Retinal Ganglion Cell Degeneration in Rats.*Oxid Med Cell Longev* 2019, 2019:8407206.
4. Park JW, Sung MS, Ha JY, Guo Y, Piao H, Heo H, Park SW: Neuroprotective Effect of Brazilian Green Propolis on Retinal Ganglion Cells in Ischemic Mouse Retina.*Curr Eye Res* 2020, 45:955-964.
5. Lin WN, Kapupara K, Wen YT, Chen YH, Pan IH, Tsai RK: Haematococcus pluvialis-Derived Astaxanthin Is a Potential Neuroprotective Agent against Optic Nerve Ischemia.*Mar Drugs* 2020, 18.
6. Guan L, Li C, Zhang Y, Gong J, Wang G, Tian P, Shen N: Puerarin ameliorates retinal ganglion cell damage induced by retinal ischemia/reperfusion through inhibiting the activation of TLR4/NLRP3 inflammasome.*Life Sci* 2020, 256:117935.
7. Wen YT, Huang TL, Huang SP, Chang CH, Tsai RK: Early applications of granulocyte colony-stimulating factor (G-CSF) can stabilize the blood-optic-nerve barrier and ameliorate inflammation in a rat model of anterior ischemic optic neuropathy (rAION).*Dis Model Mech* 2016, 9:1193-1202.
8. Melamed S: Neuroprotective properties of a synthetic docosanoid, unoprostone isopropyl: clinical benefits in the treatment of glaucoma.*Drugs Exp Clin Res* 2002, 28:63-73.
9. Georgiou T, Wen YT, Chang CH, Kolovos P, Kalogerou M, Prokopiou E, Neokleous A, Huang CT, Tsai RK: Neuroprotective Effects of Omega-3 Polyunsaturated Fatty Acids in a Rat Model of Anterior Ischemic Optic Neuropathy.*Invest Ophthalmol Vis Sci* 2017, 58:1603-1611.

10. Nguyen Ngo Le MA, Wen YT, Ho YC, Kapupara K, Tsai RK: Therapeutic Effects of Puerarin Against Anterior Ischemic Optic Neuropathy Through Antiapoptotic and Anti-Inflammatory Actions.*Invest Ophthalmol Vis Sci* 2019, 60:3481-3491.
11. Huang TL, Wen YT, Chang CH, Chang SW, Lin KH, Tsai RK: Early Methylprednisolone Treatment Can Stabilize the Blood-Optic Nerve Barrier in a Rat Model of Anterior Ischemic Optic Neuropathy (rAION).*Invest Ophthalmol Vis Sci* 2017, 58:1628-1636.
12. Kapupara K, Wen YT, Tsai RK, Huang SP: Soluble P-selectin promotes retinal ganglion cell survival through activation of Nrf2 signaling after ischemia injury.*Cell Death Dis* 2017, 8:e3172.
13. Goldenberg-Cohen N, Avraham-Lubin BC, Sadikov T, Askenasy N: Effect of coadministration of neuronal growth factors on neuroglial differentiation of bone marrow-derived stem cells in the ischemic retina.*Invest Ophthalmol Vis Sci* 2014, 55:502-512.
14. Ribas VT, Koch JC, Michel U, Bähr M, Lingor P: Attenuation of Axonal Degeneration by Calcium Channel Inhibitors Improves Retinal Ganglion Cell Survival and Regeneration After Optic Nerve Crush.*Mol Neurobiol* 2017, 54:72-86.
15. Mehrabian Z, Guo Y, Weinreich D, Bernstein SL: Oligodendrocyte death, neuroinflammation, and the effects of minocycline in a rodent model of nonarteritic anterior ischemic optic neuropathy (rNAION).*Mol Vis* 2017, 23:963-976.
16. Huang TL, Wen YT, Chang CH, Chang SW, Lin KH, Tsai RK: Efficacy of Intravitreal Injections of Triamcinolone Acetonide in a Rodent Model of Nonarteritic Anterior Ischemic Optic Neuropathy.*Invest Ophthalmol Vis Sci* 2016, 57:1878-1884.
17. Tsai RK, Chang CH, Sheu MM, Huang ZL: Anti-apoptotic effects of human granulocyte colony-stimulating factor (G-CSF) on retinal ganglion cells after optic nerve crush are PI3K/AKT-dependent.*Exp Eye Res* 2010, 90:537-545.
18. Ghalaut PS, Sen R, Dixit G: Role of granulocyte colony stimulating factor (G-CSF) in chemotherapy induced neutropenia.*J Assoc Physicians India* 2008, 56:942-944.
19. Ghahari L, Safari M, Rahimi Jaberi K, Jafari B, Safari K, Madadian M: Mesenchymal Stem Cells with Granulocyte Colony-Stimulating Factor Reduce Stress Oxidative Factors in Parkinson's Disease.*Iran Biomed J* 2020, 24:89-98.
20. Wu CC, Wang IF, Chiang PM, Wang LC, Shen CJ, Tsai KJ: G-CSF-mobilized Bone Marrow Mesenchymal Stem Cells Replenish Neural Lineages in Alzheimer's Disease Mice via CXCR4/SDF-1 Chemotaxis.*Mol Neurobiol* 2017, 54:6198-6212.
21. Lee ST, Chu K, Jung KH, Ko SY, Kim EH, Sinn DI, Lee YS, Lo EH, Kim M, Roh JK: Granulocyte colony-stimulating factor enhances angiogenesis after focal cerebral ischemia.*Brain Res* 2005, 1058:120-128.
22. Bu P, Basith B, Stubbs EB, Jr., Perlman JI: Granulocyte colony-stimulating factor facilitates recovery of retinal function following retinal ischemic injury.*Exp Eye Res* 2010, 91:104-106.
23. Popa-Wagner A, Stocker K, Balseanu AT, Rogalewski A, Diederich K, Minnerup J, Margaritescu C, Schabitz WR: Effects of granulocyte-colony stimulating factor after stroke in aged rats.*Stroke* 2010,

41:1027-1031.

24. Dwivedi P, Greis KD: Granulocyte colony-stimulating factor receptor signaling in severe congenital neutropenia, chronic neutrophilic leukemia, and related malignancies.*Exp Hematol* 2017, 46:9-20.
25. Laboissonniere LA, Goetz JJ, Martin GM, Bi R, Lund TJS, Ellson L, Lynch MR, Mooney B, Wickham H, Liu P, et al: Molecular signatures of retinal ganglion cells revealed through single cell profiling.*Sci Rep* 2019, 9:15778.
26. Ueno S, Yoneshige A, Koriyama Y, Hagiyama M, Shimomura Y, Ito A: Early Gene Expression Profile in Retinal Ganglion Cell Layer After Optic Nerve Crush in Mice.*Invest Ophthalmol Vis Sci* 2018, 59:370-380.
27. Bernstein SL, Guo Y, Kelman SE, Flower RW, Johnson MA: Functional and cellular responses in a novel rodent model of anterior ischemic optic neuropathy.*Invest Ophthalmol Vis Sci* 2003, 44:4153-4162.
28. Buschmann T, Lin Y, Aithmitti N, Fuchs SY, Lu H, Resnick-Silverman L, Manfredi JJ, Ronai Z, Wu X: Stabilization and activation of p53 by the coactivator protein TAFII31.*J Biol Chem* 2001, 276:13852-13857.
29. Uesugi M, Nyanguile O, Lu H, Levine AJ, Verdine GL: Induced alpha helix in the VP16 activation domain upon binding to a human TAF.*Science* 1997, 277:1310-1313.
30. Jabbur JR, Tabor AD, Cheng X, Wang H, Uesugi M, Lozano G, Zhang W: Mdm-2 binding and TAF(II)31 recruitment is regulated by hydrogen bond disruption between the p53 residues Thr18 and Asp21.*Oncogene* 2002, 21:7100-7113.
31. Liu PK, Wen YT, Lin W, Kapupara K, Tai M, Tsai RK: Neuroprotective effects of low-dose G-CSF plus meloxicam in a rat model of anterior ischemic optic neuropathy.*Sci Rep* 2020, 10:10351.
32. Frontini M, Soutoglou E, Argentini M, Bole-Feysot C, Jost B, Scheer E, Tora L: TAF9b (formerly TAF9L) is a bona fide TAF that has unique and overlapping roles with TAF9.*Mol Cell Biol* 2005, 25:4638-4649.
33. Fook-Alves VL, de Oliveira MB, Zanatta DB, Strauss BE, Colleoni GW: TP53 Regulated Inhibitor of Apoptosis 1 (TRIAP1) stable silencing increases late apoptosis by upregulation of caspase 9 and APAF1 in RPMI8226 multiple myeloma cell line.*Biochim Biophys Acta* 2016, 1862:1105-1110.
34. Bosco-Clément G, Zhang F, Chen Z, Zhou HM, Li H, Mikami I, Hirata T, Yagui-Beltran A, Lui N, Do HT, et al: Targeting Gli transcription activation by small molecule suppresses tumor growth.*Oncogene* 2014, 33:2087-2097.
35. Huang TL, Huang SP, Chang CH, Lin KH, Chang SW, Tsai RK: Protective effects of systemic treatment with methylprednisolone in a rodent model of non-arteritic anterior ischemic optic neuropathy (rAION).*Exp Eye Res* 2015, 131:69-76.
36. Hampsey M: Molecular genetics of the RNA polymerase II general transcriptional machinery.*Microbiol Mol Biol Rev* 1998, 62:465-503.
37. Huh JR, Park JM, Kim M, Carlson BA, Hatfield DL, Lee BJ: Recruitment of TBP or TFIIB to a promoter proximal position leads to stimulation of RNA polymerase II transcription without activator proteins

both in vivo and in vitro.*Biochem Biophys Res Commun* 1999, 256:45-51.

38. Wu SY, Chiang CM: TATA-binding protein-associated factors enhance the recruitment of RNA polymerase II by transcriptional activators.*J Biol Chem* 2001, 276:34235-34243.
39. Klaus ES, Gonzalez NH, Bergmann M, Bartkuhn M, Weidner W, Kliesch S, Rathke C: Murine and Human Spermatids Are Characterized by Numerous, Newly Synthesized and Differentially Expressed Transcription Factors and Bromodomain-Containing Proteins.*Biol Reprod* 2016, 95:4.
40. Deato MD, Marr MT, Sottero T, Inouye C, Hu P, Tjian R: MyoD targets TAF3/TRF3 to activate myogenin transcription.*Mol Cell* 2008, 32:96-105.
41. Deato MD, Tjian R: Switching of the core transcription machinery during myogenesis.*Genes Dev* 2007, 21:2137-2149.
42. Deato MD, Tjian R: An unexpected role of TAFs and TRFs in skeletal muscle differentiation: switching core promoter complexes.*Cold Spring Harb Symp Quant Biol* 2008, 73:217-225.
43. Dikstein R, Zhou S, Tjian R: Human TAFII 105 is a cell type-specific TFIID subunit related to hTAFII130.*Cell* 1996, 87:137-146.
44. Martianov I, Brancorsini S, Gansmuller A, Parvinen M, Davidson I, Sassone-Corsi P: Distinct functions of TBP and TLF/TRF2 during spermatogenesis: requirement of TLF for heterochromatic chromocenter formation in haploid round spermatids.*Development* 2002, 129:945-955.
45. Ribeiro JR, Lovasco LA, Vanderhyden BC, Freiman RN: Targeting TBP-Associated Factors in Ovarian Cancer.*Front Oncol* 2014, 4:45.
46. Bell B, Scheer E, Tora L: Identification of hTAF(II)80 delta links apoptotic signaling pathways to transcription factor TFIID function.*Mol Cell* 2001, 8:591-600.
47. Resnick MA, Tomso D, Inga A, Menendez D, Bell D: Functional diversity in the gene network controlled by the master regulator p53 in humans.*Cell Cycle* 2005, 4:1026-1029.
48. Adams C, Cazzanelli G, Rasul S, Hitchinson B, Hu Y, Coombes RC, Raguz S, Yagüe E: Apoptosis inhibitor TRIAP1 is a novel effector of drug resistance.*Oncol Rep* 2015, 34:415-422.
49. Staib F, Robles AI, Varticovski L, Wang XW, Zeeberg BR, Sirotin M, Zhurkin VB, Hofseth LJ, Hussain SP, Weinstein JN, et al: The p53 tumor suppressor network is a key responder to microenvironmental components of chronic inflammatory stress.*Cancer Res* 2005, 65:10255-10264.
50. Andrysik Z, Kim J, Tan AC, Espinosa JM: A genetic screen identifies TCF3/E2A and TRIAP1 as pathway-specific regulators of the cellular response to p53 activation.*Cell Rep* 2013, 3:1346-1354.
51. Potting C, Tatsuta T, König T, Haag M, Wai T, Aaltonen MJ, Langer T: TRIAP1/PRELI complexes prevent apoptosis by mediating intramitochondrial transport of phosphatidic acid.*Cell Metab* 2013, 18:287-295.
52. Miliara X, Garnett JA, Tatsuta T, Abid Ali F, Baldie H, Pérez-Dorado I, Simpson P, Yague E, Langer T, Matthews S: Structural insight into the TRIAP1/PRELI-like domain family of mitochondrial phospholipid transfer complexes.*EMBO Rep* 2015, 16:824-835.

Figures

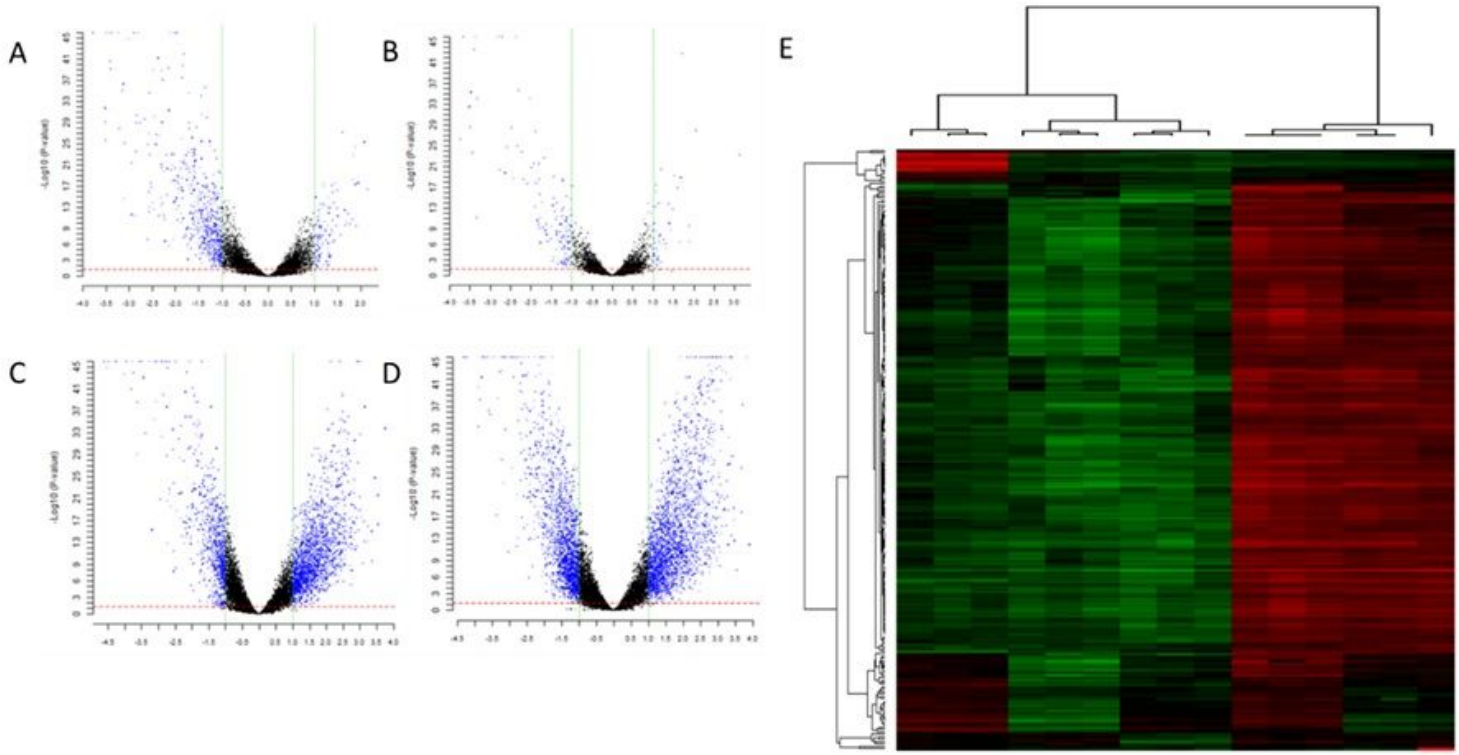

Figure 1

Gene expression profiles of the retina samples. (A-D) Volcano plot showing the differentially expressed genes in the PBS- and GCSF-treated groups. (A) The PBS-treated group (day 3 post rAION) vs. the sham-operated group. (B) The PBS-treated group (day 7 post rAION) vs. the sham-operated group. (C) The GCSF-treated group (day 3 post rAION) vs. the sham-operated group. (D) The GCSF-treated group (day 7 post rAION) vs. the sham-operated group. For each plot, the X-axis represents log2 FC, and the Y-axis represents -log10 (P-values). The differentially expressed genes are shown as red dots. (E) Hierarchical clustering of the differentially expressed genes. Up- and downregulated genes are represented in red and green colors, respectively. The differentially expressed genes were defined as having absolute FC > 1.5 and FDR < 0.1.

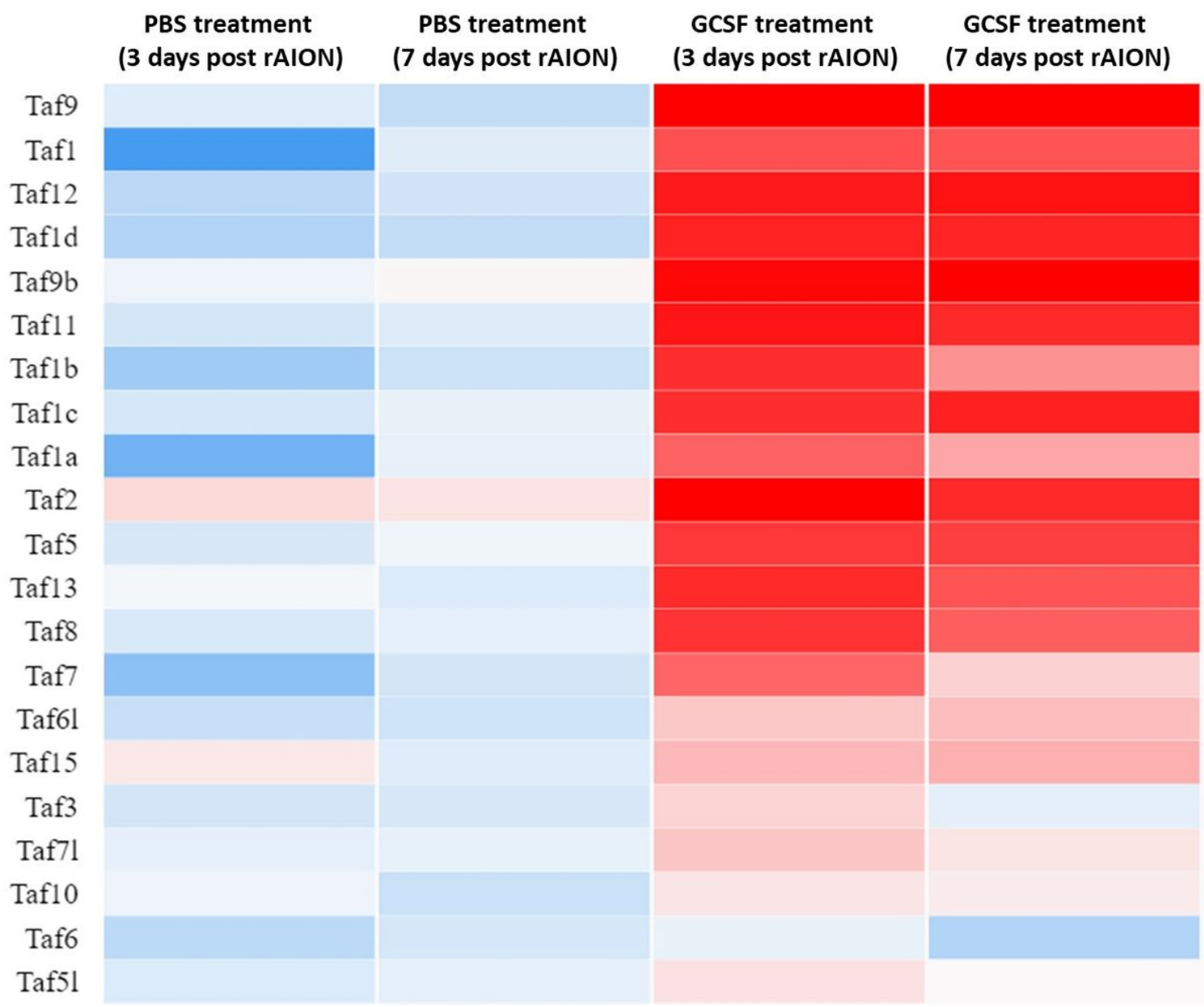

Figure 2

Heatmap of TBP-associated factors expressed in retina samples. After ON infarct, 18 TBP-associated factors were upregulated by GCSF treatment. There were 17 TBP-associated factors that were downregulated by PBS treatment. Genes were clustered into the regulation of cell survival based on gene expression over time. Up- and downregulation are represented in red and blue colors, respectively.

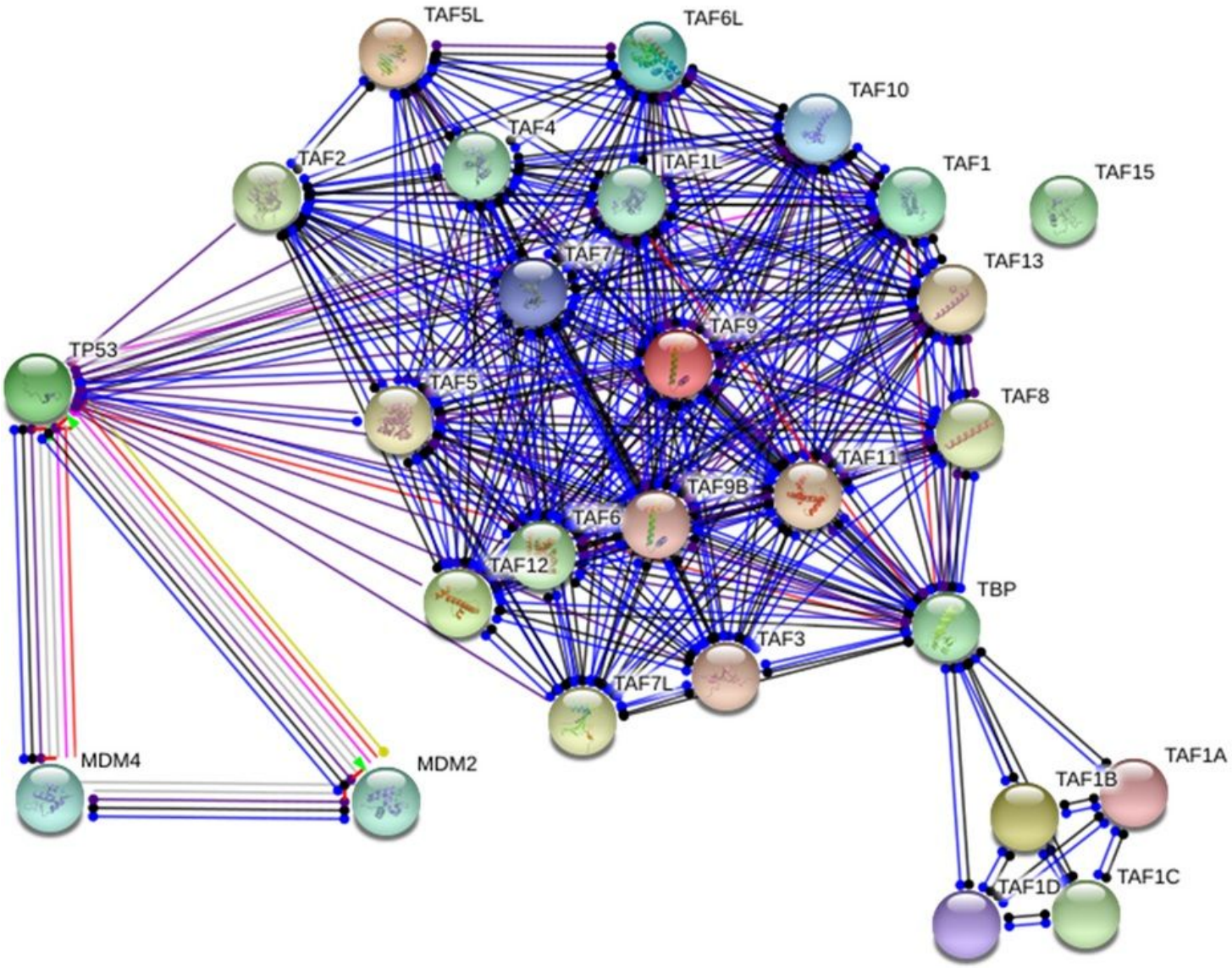

Figure 3

Network analysis of TBP-associated factors. STRING analysis shows that the TBP-associated factors are involved in the known and predicted protein-protein interactions. Network analysis exhibited that many TBP-associated factors directly interact with TP53.

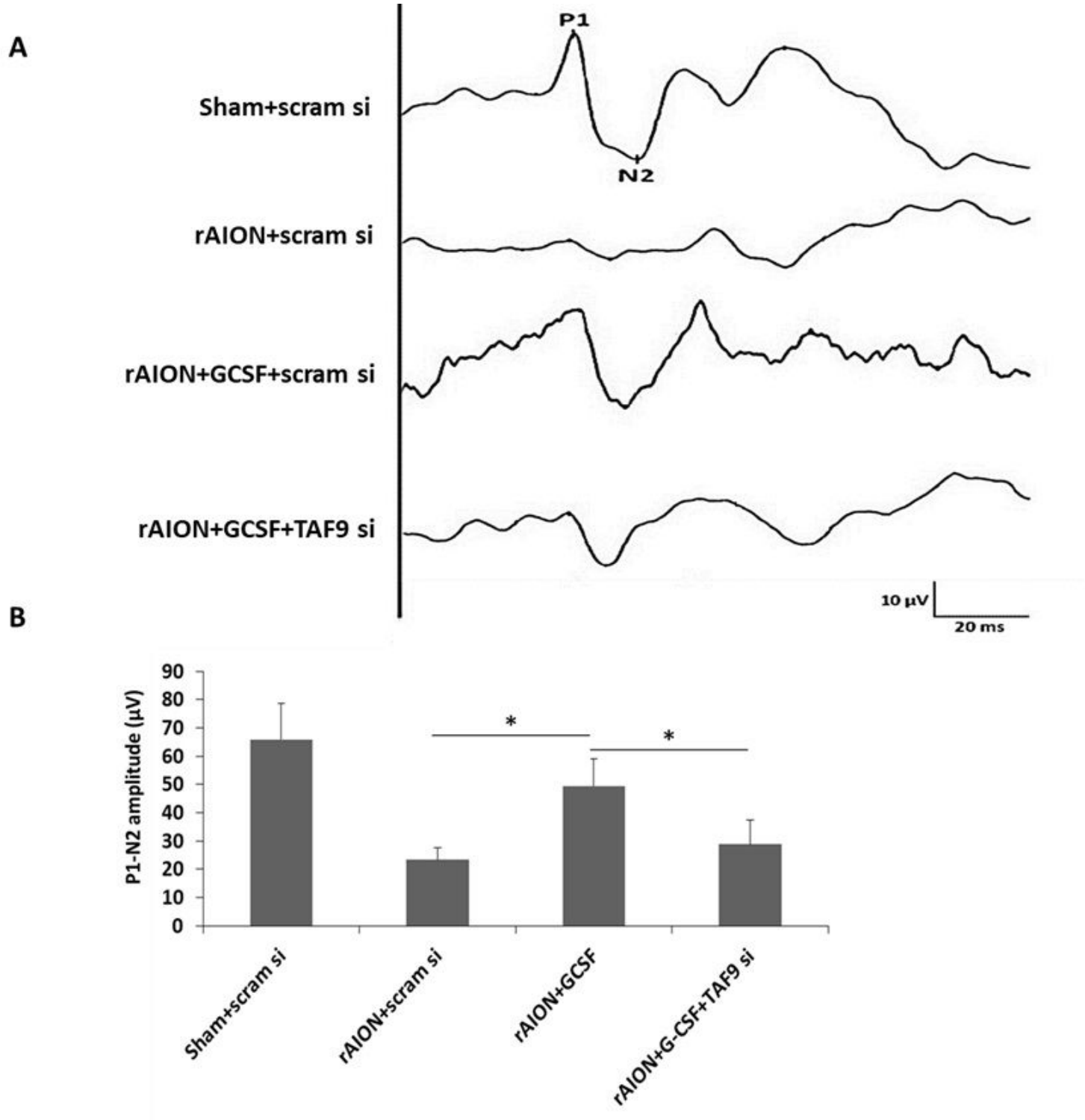

Figure 4

Effect of TAF9 knockdown on FVEP recording in the fourth week after infarct. (A) Representative FVEP wavelet in each group. (B) GCSF plus TAF9 siRNA treatment reduced the P1-N2 amplitude by 1.71-fold compared to GCSF plus scramble siRNA treatment (* $p < 0.05$, $n = 12$ per group). Data are expressed as mean ± SD.

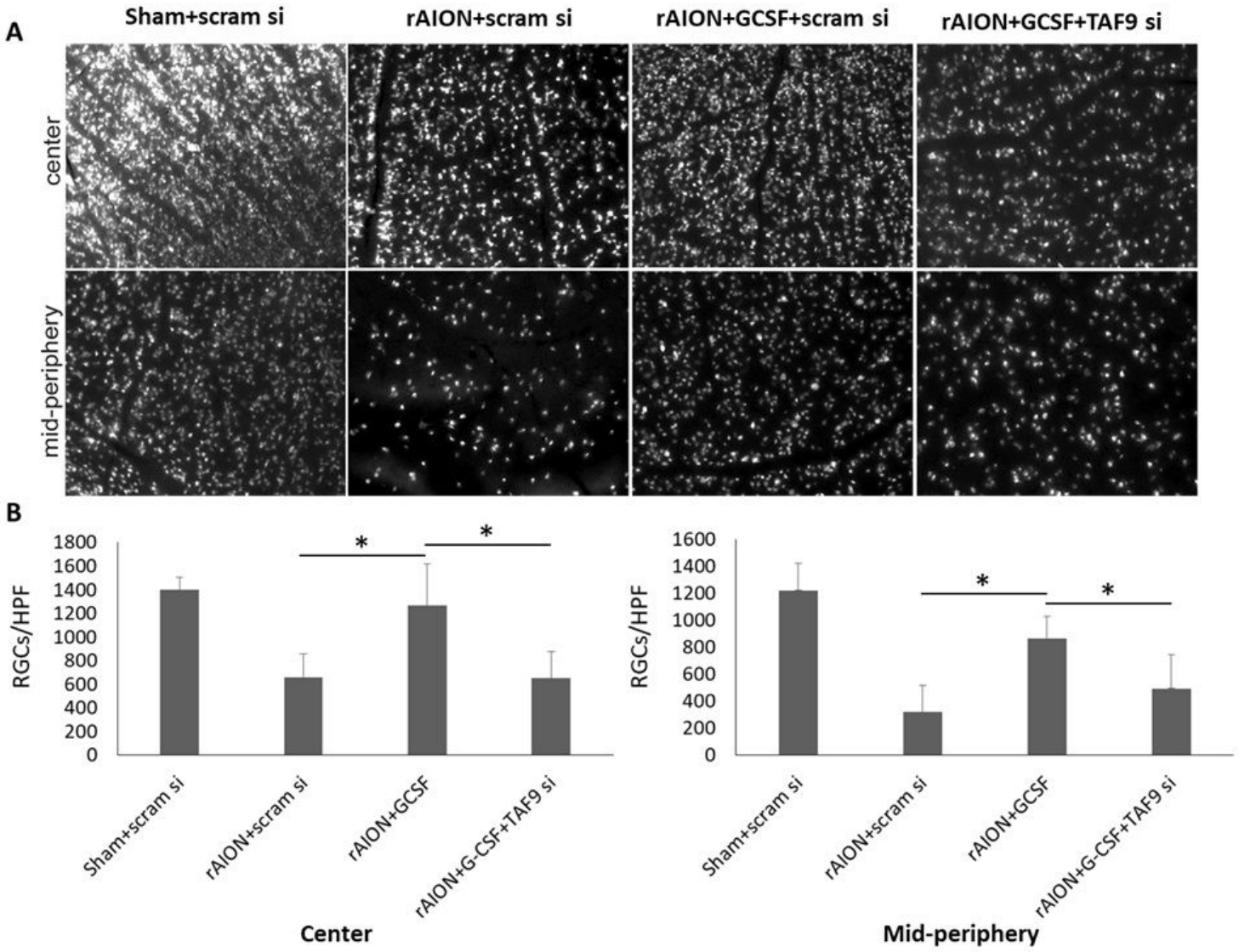

Figure 5

Effect of TAF9 knockdown on morphometry of RGCs in the fourth week after infarct. (A) Representative RGC density of the central and midperipheral retinas in each group. (B) Bar chart showing the RGC density in the GCSF plus TAF9 siRNA-treated group was significantly reduced in the central and midperipheral retinas compared to that in the GCSF plus scramble siRNA-treated group (* $p < 0.05$, $n = 12$ per group; scale bar = 50 μm).

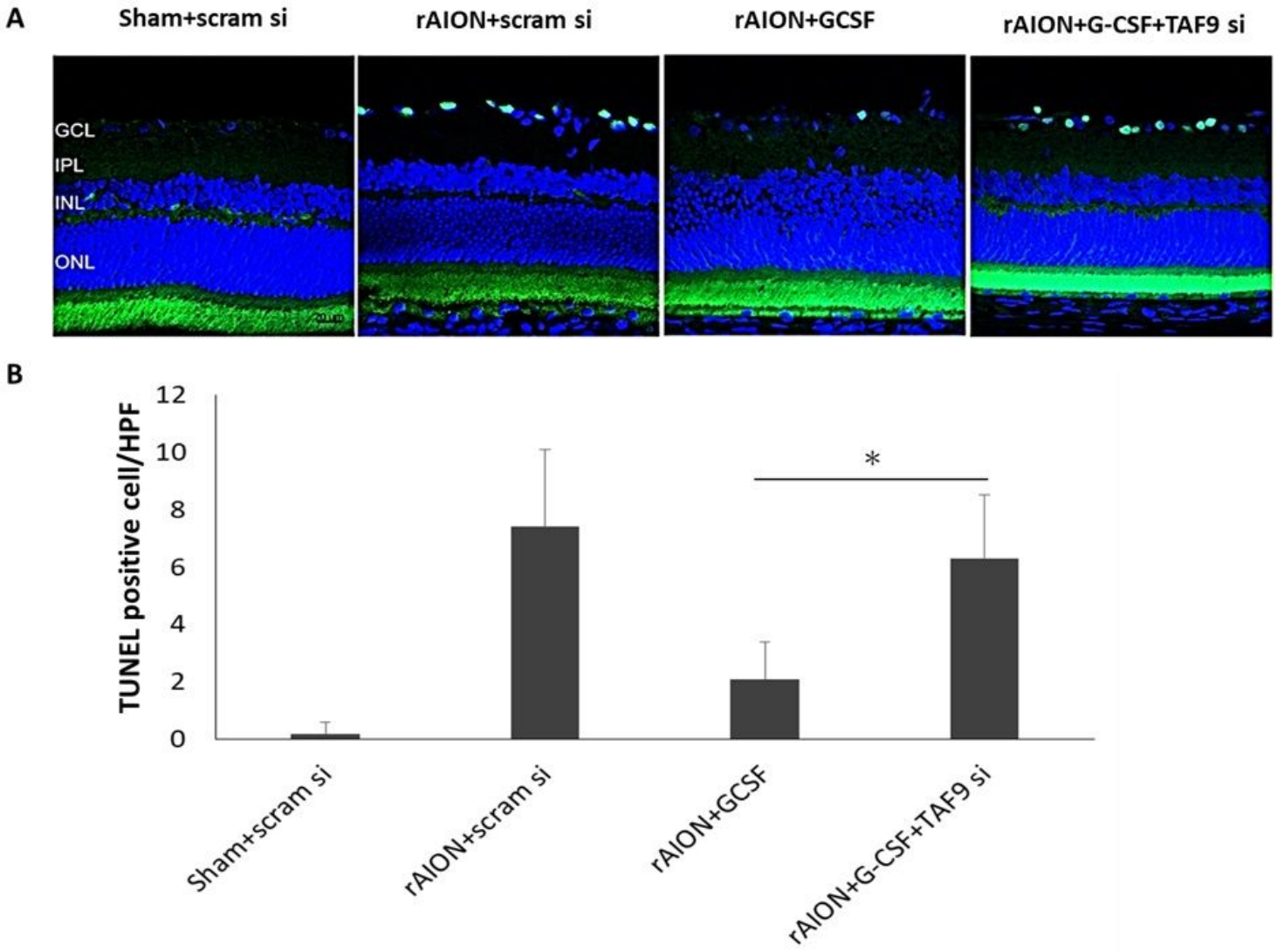

Figure 6

Analysis of RGC apoptosis in the RGC layer through the TUNEL assay in the fourth week after rAION induction. (A) Representative image of TUNEL staining. (B) Quantification of apoptotic cells per HPF. The number of TUNEL+ cell in the GCSF plus TAF9 siRNA-treated group significantly increased by threefold compared to that in the GCSF plus scramble siRNA-treated group (* $p < 0.05$, $n = 6$; scale bar = 50 μm).

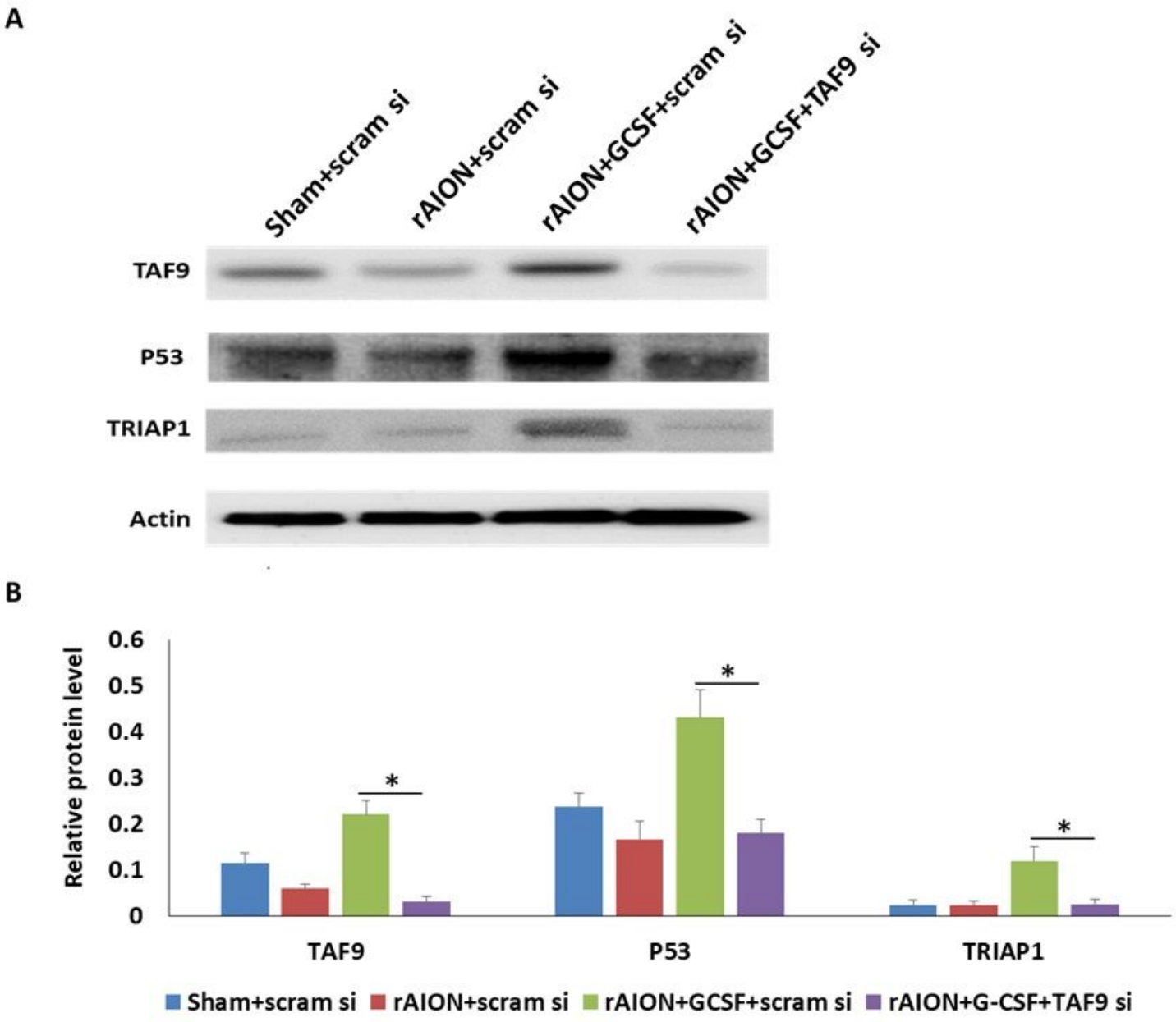

Figure 7

Western blot analysis of TAF9, TP53, and TRIAP1 expression. Treatment with GCSF plus TAF9 siRNA significantly repressed TAF9, TP53, and TRIAP1 expression by 6.9-, 2.2-, and 4.7-fold compared to treatment with GCSF plus scramble siRNA ($p < 0.05$).

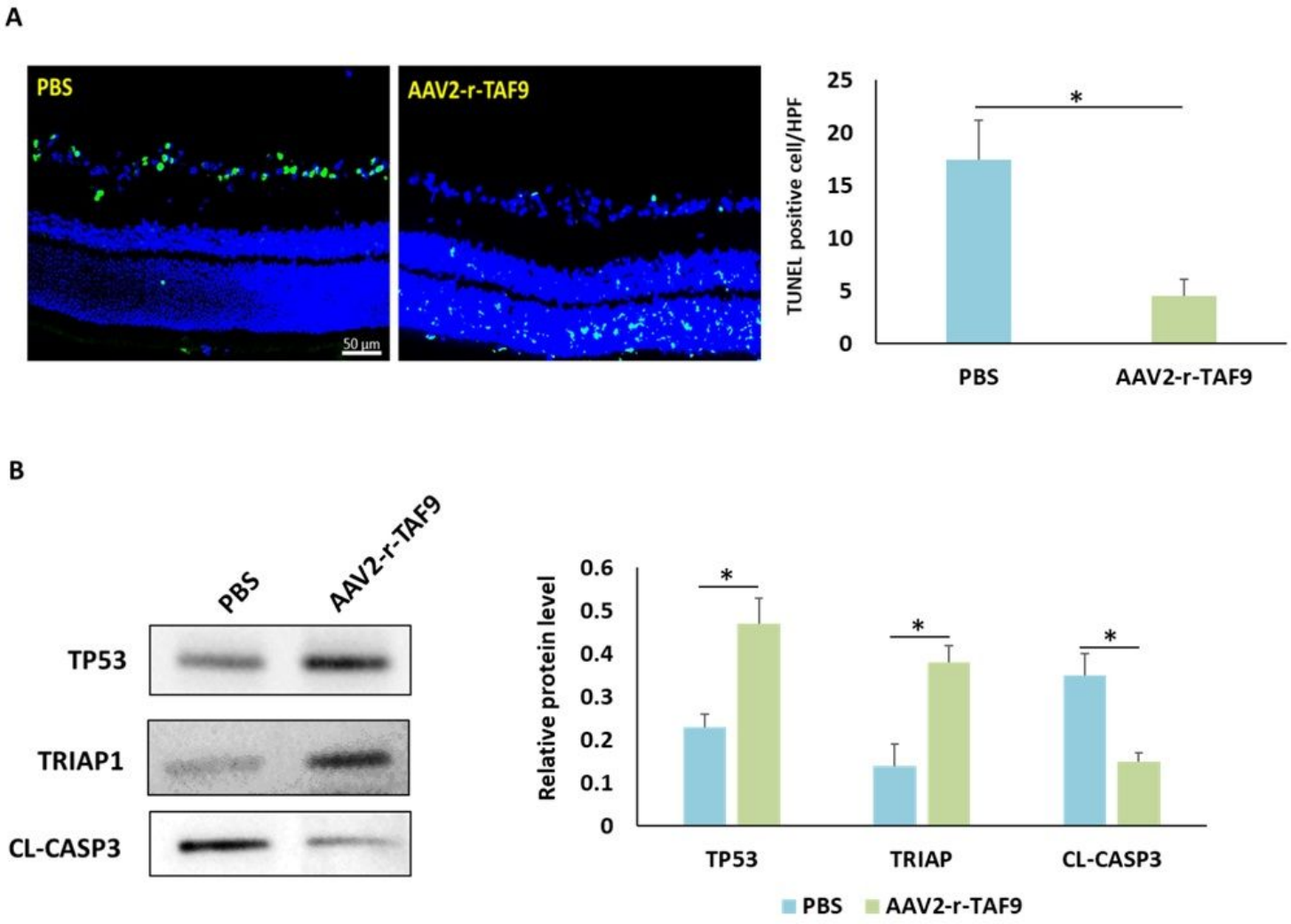

Figure 8

Effects of TAF9 overexpression on RGC apoptosis induced by rAION induction. (A) Analysis of RGC apoptosis between the PBS- and AAV2-TAF9-treated groups. (B) Western blot analysis of TP53, TRIAP1, and CASP3 expressions in the PBS- and AAV2-r-TAF9-treated groups.

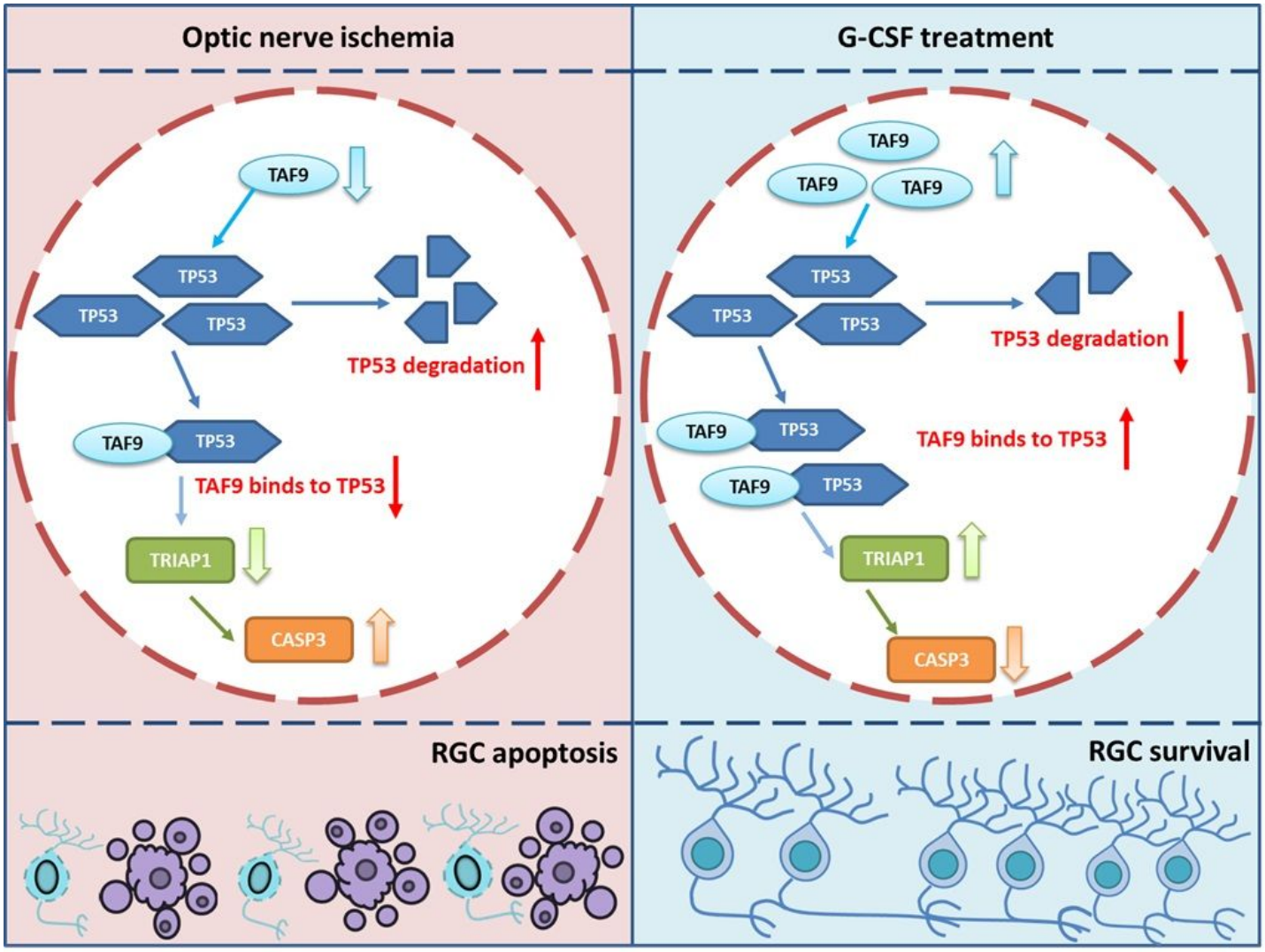

Figure 9

The graphic summary of protective mechanisms of GCSF treatment after ON infarct. GCSF treatment induced the level of TAF9. An increase of TAF9 can prevent TP53 degradation via direct binding action. The complex of TAF9 and TP53 can induce the level of TRIAP1. TRIAP1 is able to inhibit the CASP3 activation to prevent RGC apoptosis in the rAION model.